ChemPubSoc Europe

DOI: 10.1002/cmdc.201600175

CHEMMEDCHEM Full Papers

Discovery of Highly Potent Dual Orexin Receptor Antagonists via a Scaffold-Hopping Approach

Bibia Heidmann,* John Gatfield, Catherine Roch, Alexander Treiber, Simone Tortoioli, Christine Brotschi, Jodi T. Williams, Martin H. Bolli, Stefan Abele, Thierry Sifferlen, François Jenck, and Christoph Boss[a]

Starting from suvorexant (trade name Belsomra), we successfully identified interesting templates leading to potent dual orexin receptor antagonists (DORAs) via a scaffold-hopping approach. Structure–activity relationship optimization allowed us not only to improve the antagonistic potency on both orexin 1 and orexin 2 receptors (Ox1 and Ox2, respectively), but also to increase metabolic stability in human liver microsomes (HLM), decrease time-dependent inhibition of cytochrome P450 (CYP) 3A4, and decrease P-glycoprotein (Pgp)-mediated efflux. Compound **80c** [{(1*S*,6*R*)-3-(6,7-difluoroquinoxalin-2-yl)-3,8-diazabicyclo[4.2.0]octan-8-yl}(4-methyl-[1,1′-biphenyl]-2-yl)methanone] is a potent and selective DORA that inhibits the stimulating effects of orexin peptides OXA and OXB at both Ox1 and Ox2. In calcium-release assays, **80c** was found to exhibit an insurmountable antagonistic profile at both Ox1 and Ox2, while displaying a sleep-promoting effect in rat and dog models, similar to that of the benchmark compound suvorexant.

Introduction

Insomnia is a medical condition characterized by difficulty to initiate and/or to maintain restorative sleep. It can lead to irritability, concentration problems, excessive fatigue, poor work performance, driving impairments, and other health problems.[1,2] The direct and indirect costs to the global economy are considered enormously high; for the US economy alone, the costs related to insomnia have been estimated to exceed $100 billion per year.[3] The physical and psychological distress of people suffering from insomnia as well as the high economic toll and the lack of treatments that do not only improve restorative sleep but that are also free of side effects such as dependency, next day impairment, and other safety concerns led to intensive research in the field of insomnia over the last decades.[4]

In 1998 two independent research groups discovered the neuropeptides orexin A and orexin B also known as hypocretin-1 and hypocretin-2.[5] Both neuropeptides are secreted by a small population of excitatory neurons located in the lateral hypothalamus where they play essential roles in hypothalamic functions.[6,7] Orexin A and orexin B were also found to bind to previously identified orphan G protein-coupled receptors, Ox1R and Ox2R (Hcrt1 and Hcrt2 receptors).[5]

[a] *Dr. B. Heidmann, Dr. J. Gatfield, Dr. C. Roch, Dr. A. Treiber, Dr. S. Tortoioli, Dr. C. Brotschi, Dr. J. T. Williams, Dr. M. H. Bolli, Dr. S. Abele, Dr. T. Sifferlen, Dr. F. Jenck, Dr. C. Boss*
Actelion Pharmaceuticals Ltd.,
Drug Discovery and Preclinical Research & Development,
Gewerbestrasse 16, 4123 Allschwil (Switzerland)
E-mail: heidmab@actelion.com

Supporting information for this article can be found under http://dx.doi.org/10.1002/cmdc.201600175: Descriptions of all biological assays, in vivo pharmacology experiments, and experimental details for the synthesis of the reported compounds.

The orexin peptides were originally identified as stimulating food consumption (orexinergic) when directly injected into the central nervous system of rodents.[8] Further studies showed that the orexin producing neurons project to widespread and diverse regions of the brain including areas that, under circadian influence, modulate the sleep wake cycle.[9,10] Both genetic and pharmacological research confirmed that the orexin system plays an important role in maintaining arousal and wakefulness in rodents, dogs and humans.[9,11–14]

It was therefore expected that pharmacological blockade of brain orexin receptors would decrease wakefulness and promote sleep by a mechanism of action very different from available drugs (i.e., GABA receptor modulators) known to suppress overall central nervous system activation through potentiation of inhibitory neurotransmission.[9] It was demonstrated that pharmacological modulation of orexin signaling with small-molecule antagonists decreases wake and induces sleep in preclinical species (rodent and canine models) and in patients suffering from insomnia.[9,15,16]

Interest in the concept of orexin receptor antagonism has been boosted in 2007 with the disclosure of almorexant **1**, an orally active dual orexin receptor antagonist (DORA) that promotes sleep in rats, dogs and in humans without evidence of cataplexy and therefore provided proof-of-concept of orexin antagonism for the treatment of primary insomnia.[16—17] More recently, Merck's DORA suvorexant **3**, which dose dependently increases total sleep time by decreasing latency to persistent sleep and wake after sleep onset, was granted US Food and Drug Administration (FDA) approval as first-in-class drug for the treatment of insomnia (Belsomra).[12b,18,19–28]

Over the past years, several high throughput screening campaigns using Ca^{2+} release assays (FLIPR) for the search of new

DORAs were performed at Actelion. They provided interesting hits that were further optimized into potent and brain penetrant DORAs.[9b,29–35] Lately, we reported on the sulfonamide ACT-462206 as preclinical candidate that emerged from those efforts.[35] With the increasing knowledge on DORA binding modes and the availability of several potent DORAs in clinical trials for primary insomnia (Figure 1), we decided to tackle the search for new lead structures via a scaffold-hopping approach using **3** as a template.[9b,26,36–41]

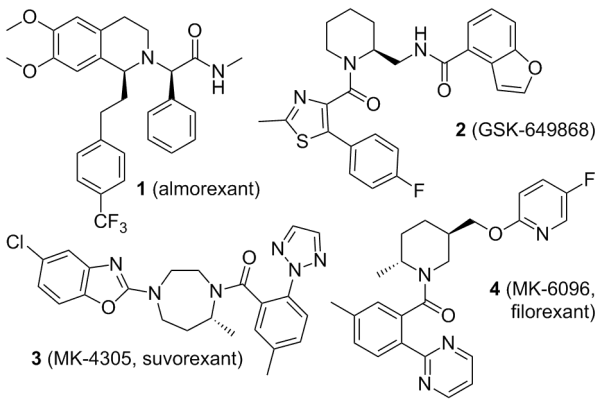

Figure 1. DORAs reported in clinical trials.

Herein we report the identification of novel starting points as dual orexin receptor antagonists following a scaffold-hopping approach. We also describe herein the structural optimization of one scaffold into an orally bioavailable and CNS penetrant DORA.

Results and Discussion

With the active conformation reported by Merck for their *N*,*N*-disubstituted-1,4-diazepane derived series, we decided to use **3** as a template for our scaffold-hopping approach to identify new starting points for the design of new DORAs.[41] Our strategy was to first retain the 5-chlorobenzo[*d*]oxazole and the (5-methyl-2-(2*H*-1,2,3-triazol-2-yl)phenyl)methanone substituents and to replace the central 1,4-diazepane ring with new bicyclic "diamine" templates (Figure 2) that allow for the same intramolecular π-stacking interaction between the substituents and the adoption of the suggested low-energy twist-boat ring bioactive conformation.[41] The final goal being to replace the peripheral substituents of **3** with proprietary substituents.

Analysis of potential templates (from commercial sources and/or described in the literature) was performed using "Chem3DPro" and "Actelion 3D Modeling" tools allowing for manual alignments of ligands of interest with selected templates. Our studies suggested that several constrained systems enforce the low energy conformation observed with diazepane **3** leading to highly potent compounds on both Ox1 and Ox2 receptors.[41] The templates' selection was based on three criteria: conformational similarity to compound **3**, freedom to operate based on published patents, and commercial availability/synthetic accessibility. In Table 1, we report the data generated in house for the benchmark compound **3**. In Tables 2–4, the identified templates fulfilling these requirements are depicted with their antagonistic potency on Ox1 and Ox2 receptors determined using FLIPR assay technology. Compounds listed in Tables 2–4 were synthesized by following the synthetic route depicted in Scheme 1 using the *cis*-3,8-diazabicyclo[4.2.0]octane template as example.[42]

Table 1. In-house data for benchmark compound **3**.

Diazepane	R^1	R^2	Compd	IC_{50} [nM][a] hOx1	hOx2
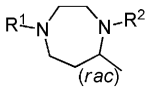 (*rac*)	A	B	**5**	1.8	5.9
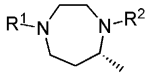	A	B	**3**	1.0	2.8
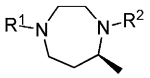	A	B	**3a**	13	58

[a] Values are the geometric mean of at least two to three independent experiments as determined by FLIPR assay (see the Supporting Information for details).

tert-Butyl 3,8-diazabicyclo[4.2.0]octane-8-carboxylate **56** can be purchased or synthesized according to known procedures.[42] Amide coupling with 5-methyl-2-(2*H*-1,2,3-triazol-2-yl)-benzoic acid **57**, followed by Boc-deprotection and nucleophilic aromatic substitution using 2,5-dichlorobenzo[*d*]oxazole **60**

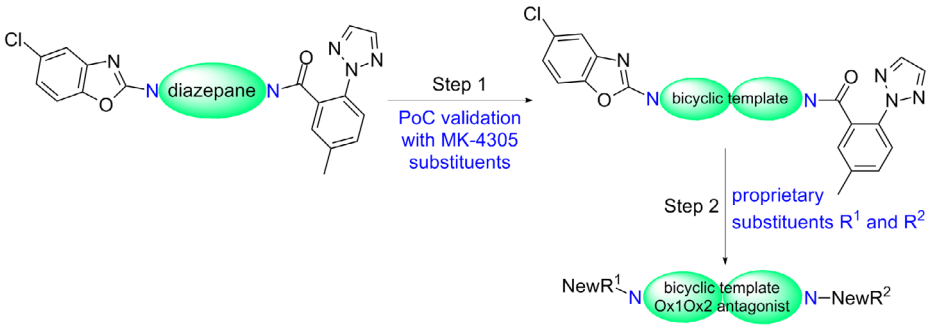

Figure 2. Scaffold hopping proof-of-concept (PoC) validation.

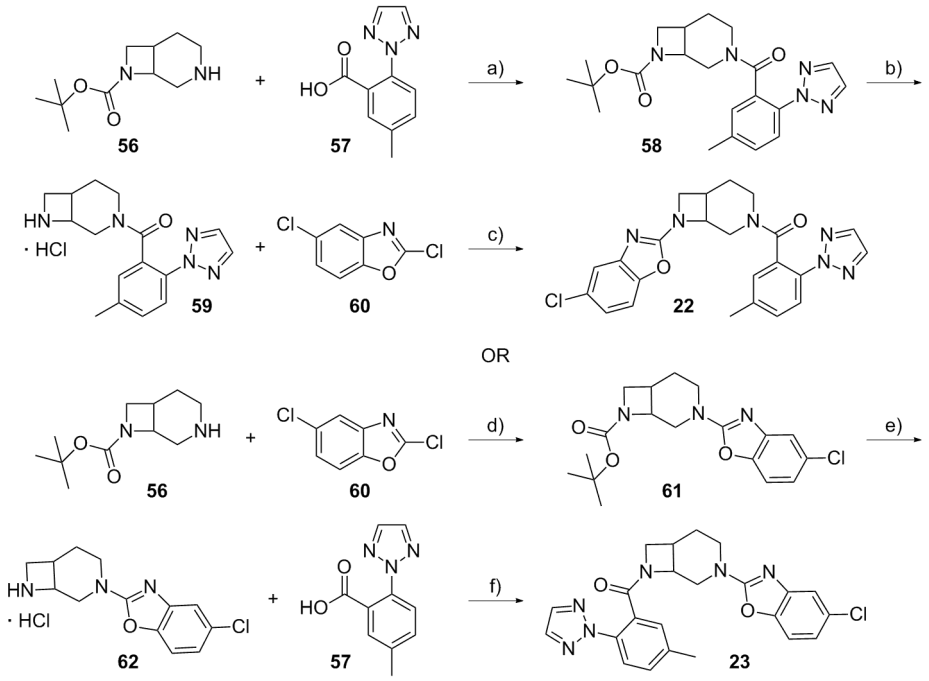

Scheme 1. Synthesis of 3,8-diazabicyclo[4.2.0]octane **22** and **23** as orexin receptor antagonists (details given in the Supporting Information). *Reagents and conditions*: a) TBTU, DIPEA, CH_3CN, RT, 17 h, 92%; b) HCl 4 N in dioxane, RT, 4 h, quant.; c) K_2CO_3, DMF, 60 °C, 17 h, 82%; d) K_2CO_3, DMF, 60 °C, 17 h, 95%; e) HCl 4 N in dioxane, RT, 4 h, quant.; f) TBTU, DIPEA, CH_3CN, RT, 17 h, 77%.

afforded the DORA **22** in Table 2. *Rac*-**22** could be resolved by chiral HPLC to afford enantiomers **22a** and **22b**.[44] The sequence was reversed in order to reach compound **23** in Table 2: **56** was treated with 2,5-dichlorobenzo[*d*]oxazole **60** followed by Boc-deprotection and amide coupling with acid **57**. As for the regioisomer *rac*-**22**, *rac*-**23** could be resolved by HPLC using a chiral stationary phase to afford enantiomers **23a** and **23b**.[45]

The fused bicyclic templates reported in Table 2 delivered several interesting scaffolds with reference compounds (**7**, **8**, **16**, **22**, and **23**) reaching potencies below 100 nM on both orexin receptors. Interestingly, the spiro scaffolds (Table 3), when active, resulted in compounds preferentially active at the Ox1 receptor (e.g., **28**, **37**, and **39**). The same was true for the bridged templates depicted in Table 4. The three most attractive scaffolds led to preferential Ox1R antagonists (**53**, **54**, and **55**).[43] Following our project's goal, we favored the scaffolds with the highest potential to deliver DORAs, with reasonable molecular weight and with a modular structure easily amenable to parallel synthesis for SAR optimization. This was the case for **7**, **8**, **16**, **22**/**23** (Table 2). Among these, we decided to concentrate our efforts on the 3,8-diazabicyclo[4.2.0]octane template (compounds **22** and **23**) that not only resulted in reference compound **22** being equally potent to compound **3**, but which can interestingly also accommodate its regioisomer **23** keeping high affinity for both orexin receptors.[42] Enantiomers **22a** and **22b** differed in receptor affinity by greater than 400-fold on both receptors in favor of the single enantiomer **22a** while enantiomers **23a** and **23b** differed in receptor affinity by greater than 50-fold on Ox1R and by greater than 190-fold on Ox2R in favor of the single enantiomer **23a**. Notably, the active enantiomer **22a** (amide on the piperidine ring) exhibits (1*R*,6*S*)-chirality, while the active enantiomer **23a** (amide on the azetidine ring) exhibits the opposite (1*S*,6*R*)-chirality (Figure 3).

To identify potential issues to be addressed prior to embarking on the SAR optimization, we examined the in vitro and the in vivo properties of **22a** and **23a**. For the in vivo experiments, all procedures were approved by the local Veterinary Office and strictly adhered to Swiss federal and international regulations on animal experimentation.

Both compounds exhibited identical physicochemical properties (Table 5). They were moderately lipophilic with Log$D_{7.4}$ of 3.2 (cLog$P$ = 4.0) with a polar surface area of 73.1 Å^2 indicating a high probability for brain penetration. Their profiles on cytochrome P450 (CYP) inhibition were similar except for the strong time-dependent CYP3A4 inhibition with a shift in IC_{50} values after pre-incubation (thereafter called "CYP3A4 shift") of 30-fold measured for **22a** as opposed to the moderate CYP3A4 shift for **23b** (4.7-fold). Both compounds were similarly bound to human plasma proteins (98%) with high passive permeability in human MDR1-MDCK cells of 86.10^{-6} and

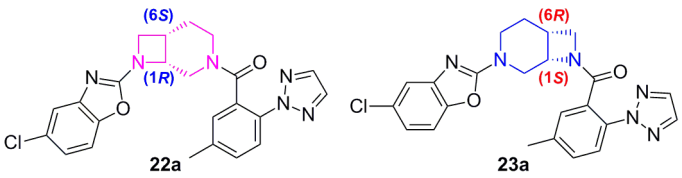

Figure 3. Stereochemistry for 3,8-diazabicyclo[4.2.0]octane active enantiomers.

Table 2. Potency obtained for selected bicyclic diamine templates: fused bicyclic templates.

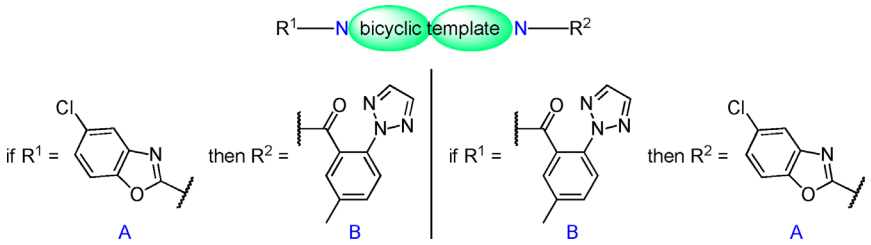

Bicyclic template	R^1	R^2	Compd	IC_{50} [nM][a] hOx1	hOx2	Stereochemistry
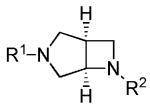	A	B	**6**	1742	3100	Racemic
	B	A	**7**	13	25	
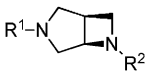	B	A	**7a**	5.1	17	Optically pure
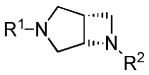	B	A	**7b**	1880	2935	Optically pure
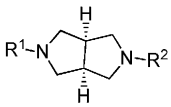	A	B	**8**	71	64	Meso
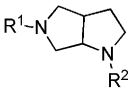	A	B	**9**	1030	544	Unknown chirality
	B	A	**10**	118	119	
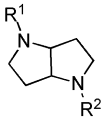	A	B	**11**	1556	2375	Unknown chirality
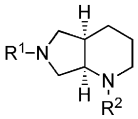	A	B	**12**	1548	528	Racemic
	B	A	**13**	2249	1118	
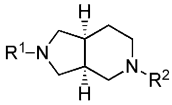	A	B	**14**	386	746	Racemic
	B	A	**15**	125	137	
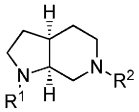	A	B	**16**	26	45	Racemic
	B	A	**17**	204	290	
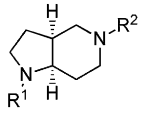	A	B	**18**	669	1048	Racemic
	B	A	**19**	1925	1315	
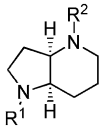	A	B	**20**	1343	915	Racemic
	B	A	**21**	2242	912	
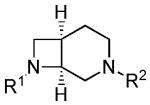	A	B	**22**	1.7	7.5	Racemic
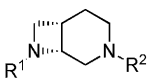	A	B	**22a**	0.9	2.9	This enantiomer

Table 2. (Continued)

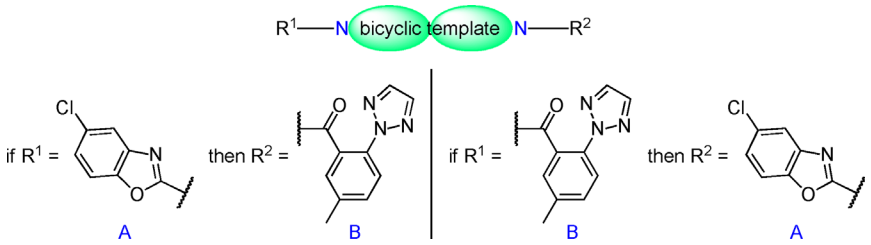

Bicyclic template	R^1	R^2	Compd	IC_{50} [nM][a] hOx1	hOx2	Stereochemistry
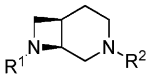	A	B	**22b**	474	1251	This enantiomer
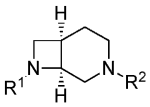	B	A	**23**	22	31	Racemic
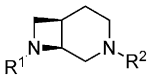	B	A	**23a**	12	17	This enantiomer
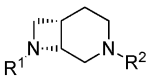	B	A	**23b**	668	3240	This enantiomer
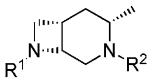	A B	B A	**24** **25**	96 840	288 369	Racemic
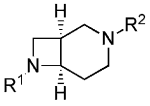	A B	B A	**26** **27**	163 359	2080 995	Racemic

[a] Values are the geometric mean of at least two to three independent experiments as determined by FLIPR assay (see the Supporting Information for details).

76.10^{-6} cm s^{-1}, respectively. Yet **22a** was a strong substrate for human P-glycoprotein (Pgp) with an efflux ratio of 11 as opposed to the moderate efflux of 4.7 measured for **23a**. Finally, **23a** was also more stable than **22a** in human and dog liver microsomes (HLM and DLM) while both compounds were highly unstable in rat liver microsomes (RLM >1250 µL min^{-1} mg^{-1}). Consistent with their relatively lipophilic nature and their high intrinsic clearance in RLM, both compounds showed moderate clearance in Wistar rats (17 and 23 mL min^{-1} kg^{-1}, Table 6) and low bioavailability ($F=8$ and 11%). Apparent terminal $t_{1/2}$ was shorter for **22a** (1.1 h) as compared to **23a** (21 h) but both compounds were quickly absorbed after oral dosing as peak drug levels were reached within the first 30 min ($t_{max}=0.5$ h). The pharmacokinetic parameters evaluated in Beagle dogs (Table 6) were similar for both compounds showing lower clearance than the rat data (9.6 and 12 mL min^{-1} kg^{-1}), similar volumes of distribution ($V_{ss}=0.8$ and 1.3 L kg^{-1}), and short $t_{1/2}$ (~1 h) even for a sleeping drug that should be cleared from the body within 6–8 h. In Beagle dogs, compound **23a** was more bioavailable than **22a** (77 vs. 58%) and was absorbed three times faster ($t_{max}=0.38$ vs. 1 h). Compounds **22a** and **23a** were further profiled in in vivo blood–brain barrier (BBB) experiments in male Wistar rats to assess their brain penetration potential. The dose used was 100 mg kg^{-1} to overcome the high first-pass metabolism in rats. As shown in Table 6, both compounds showed excellent total brain concentrations of [B] = 2741 and 3394 ng g^{-1} for **22a** and **23a**, respectively. Based on the high total brain concentrations, both compounds were evaluated for their sleep-promoting effects in male Wistar rats equipped with radiotelemetry probes continuously recording electroencephalogram/electromyography (EEG/EMG) and locomotor activity. The animals were administered with a single oral dose of 100 mg kg^{-1} at the beginning of the nocturnal active phase, when endogenous orexin levels increase. All experiments where done in a crossover design. Over the 12 h night period following administration, both **22a** and **23a** significantly decreased the home cage activity by 31 and 32% relative to their respective vehicle-treated rats ($p<0.001$ for both, paired *t*-test). Electrophysiologically **22a** slightly but not significantly decreased the time spent in active wake and quiet wake (−9 and −5%, respectively; $p>0.05$, paired *t*-test; Figure 4). The time spent in non-REM (rapid eye movement) sleep increased significantly by 10% ($p<0.05$, paired *t*-test) and the time spent in REM sleep increased not significantly by 20% relative to vehicle-treated rats ($p<0.05$, paired *t*-test; Figure 4). The total

Table 3. Potency obtained for selected bicyclic diamine templates: spiro templates.

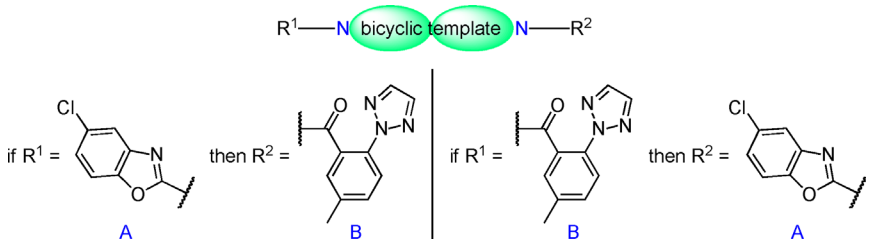

Bicyclic Template	R^1	R^2	Compd	IC_{50} [nM][a] hOx1	hOx2	Stereochemistry
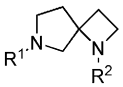	A	B	**28**	127	1253	Racemic
	B	A	**29**	1403	1008	
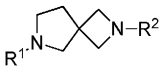	A	B	**30**	1643	1415	Racemic
	B	A	**31**	464	722	
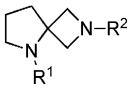	A	B	**32**	281	117	Racemic
	B	A	**33**	291	528	
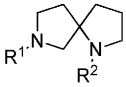	A	B	**34**	1270	392	Racemic
	B	A	**35**	892	895	
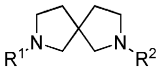	A	B	**36**	494	955	Racemic
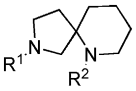	A	B	**37**	1.4	47	Racemic
	B	A	**38**	292	1200	
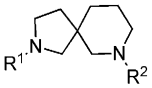	A	B	**39**	8.6	514	Racemic
	B	A	**40**	212	1039	
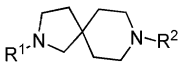	A	B	**41**	1270	2350	Racemic
	B	A	**42**	1190	960	
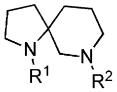	A	B	**43**	2223	1858	Racemic
	B	A	**44**	1087	1451	

[a] Values are the geometric mean of at least two to three independent experiments as determined by FLIPR assay (see the Supporting Information for details).

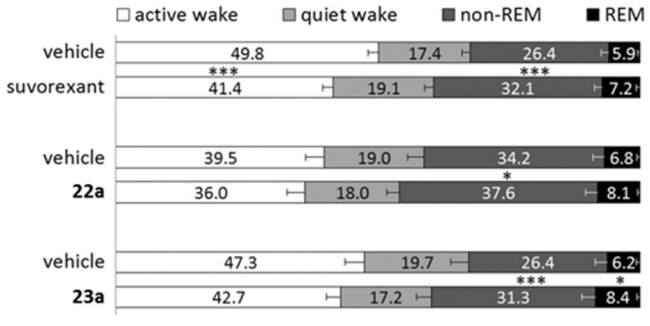

Figure 4. All experiments were done in a crossover design. Effect of **22a**, **23a**, and suvorexant **3** on the time spent in sleep and wake stages (percent of total time) during the 12 h night active period following administration in male Wistar rats. Rats were administered a single oral dose of vehicle or compound (100 mg kg^{-1}). Data are presented as mean ± SEM; *$p < 0.05$, ***$p < 0.001$ ($n = 7$ for **22a**, $n = 8$ for **23a** and $n = 14$ for suvorexant **3**).

sleeping time increased by 12% relative to the vehicle-treated rats and the relative proportion of the time spent in non-REM and REM sleep was stable (82 and 18% of non-REM and REM sleep, respectively, for the **22a**-treated rats compared with the 83 and 17% non-REM and REM sleep for the vehicle-treated rats ($p > 0.05$, paired *t*-test). Based on its high potency on both orexin receptors and its unbound brain concentration ($[B]_u =$ 67 nM $\sim 56 \times IC_{50\ rOx2}/35 \times IC_{50\ rOx1}$), **22a** was expected to be more active and to show a similar sleep-promoting effect as our benchmark suvorexant **3**, which under the same experimental conditions, increased the total sleep time by 22% over the vehicle-treated rats. Contrasting effects were observed with **23a** which showed good efficacy despite lower potency on both orexin receptors and lower unbound brain concentration, when reported to the potency on both receptors ($[B]_u =$ 129 nM $\sim 15 \times IC_{50\ rOx2}/4 \times IC_{50\ rOx1}$), than **22a**. It decreased slightly and not significantly the time spent in active wake and

Table 4. Potency obtained for selected bicyclic diamine templates: monocyclic and bridged templates.

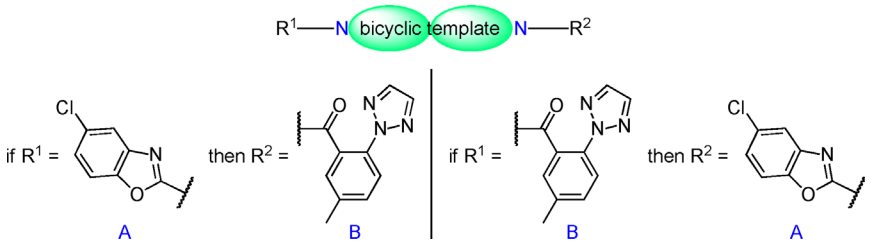

Template	R^1	R^2	Compd	IC_{50} [nM][a] hOx1	hOx2	Stereochemistry
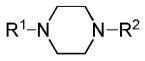	A	B	**45**	1651	1831	None
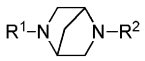	A	B	**46**	1473	883	Racemic
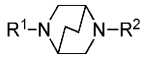	A	B	**47**	277	650	Racemic
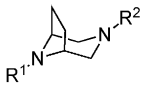	A B	B A	**48** **49**	464 2017	153 2009	Racemic
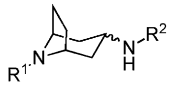	A B	B A	**50** **51**	2032 2403	753 1670	Unknown chirality
	A B	B A	**52** **53**	583 17	3367 223	Unknown chirality
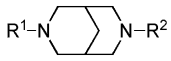	A	B	**54**	6.5	542	Meso
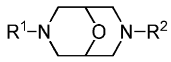	A	B	**55**	163	>6460	Meso

[a] Values are the geometric mean of at least two to three independent experiments as determined by FLIPR assay (see the Supporting Information for details).

quiet wake relative to vehicle-treated rats (−10 and −13%, respectively; $p > 0.05$, paired *t*-test) but increased significantly both the time spent in non-REM sleep (+18% compared with vehicle-treated rats; $p < 0.001$, paired *t*-test) and the time spent in REM sleep (+37% compared with vehicle-treated rats; $p < 0.05$, paired *t*-test; Figure 4). The total sleeping time increased by 22% relative to the vehicle-treated rats. These effects were similar to those observed with benchmark compound **3**.

The data compiled in Tables 5 and 6 were clearly in favor of compound **23a**, which showed a lower shift in the time-dependent CYP3A4 inhibition assay and a much lower Pgp efflux than **22a**. Moreover **22a**, despite its high unbound brain concentration and high potency on both orexin receptors, was surprisingly poorly active in the EEG/EMG in vivo experiment contrasting with **23a** that showed effects similar to those observed with compound **3**.

We therefore decided to concentrate our SAR efforts on the template (1*S*,6*R*)-3,8-diazabicyclo[4.2.0]octane with the amide bound to the azetidine ring and the aromatic substituent at the piperidine ring.[46] In addition to improving the potency on both orexin receptors, our main goal was to decrease the Pgp efflux ratio to values below three. In view of the targeted clinical indication we also aimed at having moderately stable compounds in HLM in order to achieve an appropriate clearance yielding to a sleep effect of 6 to 8 h in humans to avoid next-day drowsiness.

Final compounds in the (1*S*,6*R*)-3,8-diazabicyclo[4.2.0]octane series were prepared according to the route depicted in Scheme 1, and the core building block was synthesized following published procedures.[42]

Our SAR work started with the goal of finding a suitable isosteric replacement for the 5-chlorobenzo[*d*]oxazole western part of **23a**. Previously reported SAR analysis on the Merck diazepam amide DORA series demonstrated that the lipophilic interactions in the 5-chlorobenzo[*d*]oxazole region are of key importance for antagonist potency.[18,39] Removal of the distal fused phenyl in the western side heterocycle leads to inactive compounds on both receptors. Therefore, we favored fused heterocycles that allow for the same level of lipophilicity in this region. We also aimed at keeping the planar topology of the fused benzo[*d*]oxazole ring. Table 7 summarizes our efforts to replace the 5-chlorobenzo[*d*]oxazole moiety.[47] All reported derivatives were assayed as racemic mixtures, except if otherwise stated. Interesting racemic mixtures with potencies below 20 nM on one receptor and at least 40 nM on the other receptor were separated by chiral HPLC for further profiling. In our

Table 5. Comparative in vitro data for **22a** and **23a**.[a]

Properties	Compound **22a**	Compound **23a**
PhysChem properties		
M_r [g mol^{-1}]	448.91	448.91
Log$D_{7.4}$	3.2	3.2
PSA [Å^2]	73.1	73.1
Human and rat orexin receptors		
IC_{50} (hOx1/rOx1) [nM]	0.9/1.9	12/35
IC_{50} (hOx2/rOx2) [nM]	2.9/1.2	17/8.6
CYP inhibition		
IC_{50} (CYP3A4T) [μM]	12	26
IC_{50} (CYP3A4M) [μM]	12	>50
CYP3A4 shift	30-fold	4.2-fold
IC_{50} (CYP2C9) [μM]	32	28
CYP2C9 shift	1	1
IC_{50} (CYP2D6) [μM]	>50	>50
CYP2D6 shift	1	1
Metabolic stability in liver microsomes		
HLM [μL min^{-1} mg^{-1}]	219	59
RLM [μL min^{-1} mg^{-1}]	>1250	>1250
DLM [μL min^{-1} mg^{-1}]	165	44
Plasma protein binding		
rat PPB [%]	98.0	98.5
Fu_rat brain	0.011	0.017
MDR1 assay		
P_{app} A→B [10^{-6} cm s^{-1}]	7.5	16
P_{app} B→A [10^{-6} cm s^{-1}]	85	76
Efflux ratio	11	4.7

[a] Orexin activity data are the geometric mean of at least two to three independent experiments and were determined by FLIPR assay (see the Supporting Information for details). CYP3A4T: testosterone as marker substrate; CYP3A4M: midazolam as marker substrate; HLM, RLM, and DLM values represent a normalized rate constant.

Table 6. Comparative in vivo data for **22a** and **23a**.[a]

Properties	Compound **22a**	Compound **23a**
Pharmacokinetics: Wistar rat, 1 mg kg^{-1} i.v.		
AUC [ng h mL^{-1}]	965	732
CL [mL min^{-1} kg^{-1}]	17	23
V_{ss} [L kg^{-1}]	0.6	1
Terminal $t_{1/2}$ [h]	1.1	21
Pharmacokinetics: Wistar rat,[a] 10 mg kg^{-1} p.o.		
AUC [ng h mL^{-1}]	770	822
C_{max} [ng mL^{-1}]	372	818
t_{max} [h]	0.5	0.5
F [%]	8	11
Pharmacokinetics: Beagle dog[b]	**1 mg kg^{-1} i.v.**	**0.3 mg kg^{-1} i.v.**
AUC [ng h mL^{-1}]	1740	416
CL [mL min^{-1} kg^{-1}]	9.6	12
V_{ss} [L kg^{-1}]	0.7	1.3
Terminal $t_{1/2}$ [h]	0.8	1.2
Pharmacokinetics: Beagle dog[b]	**5 mg kg^{-1} p.o.**	**3 mg kg^{-1} p.o.**
AUC [ng h mL^{-1}]	5050	3190
C_{max} [ng mL^{-1}]	1400	936
t_{max} [h]	1	0.4
F [%]	58	77
Blood–brain barrier (BBB) experiments:[c] total values		
[B] [ng g^{-1}]	2741	3394
[P] [ng mL^{-1}]	4973	8488
[CSF] [ng mL^{-1}]	191	247
[B]/[P] ratio [%]	55	40

[a] Data are the geometric mean; the median is given for t_{max}. [b] For formulation details see the experimental section in the Supporting Information. [c] Administered at 100 mg kg^{-1} p.o. in male Wistar rats (see experimental details in the Supporting Information). Sampling at t = 3 h post-dosing; formulation in PEG400.

screening cascade, metabolic stability in HLM was assessed first, followed by the time-dependent CYP3A4 inhibition and eventually permeability and active transport in a human MDR1-MDCK assay. Indeed, these key properties for a sleeping drug were identified as potential liabilities in the lead compound **23a**. Thus for HLM values below 500 μL min^{-1} mg^{-1}, the compounds were further tested in the time-dependent CYP3A4 inhibition assay and only those with a shift lower than 5 were tested in the in vitro Pgp assay.

Benzo[*d*]oxazoles led to poorly or moderately active compounds as illustrated by the 5-fluoro-benzo[*d*]oxazole present in **63**. More active compounds were obtained when the benzo[*d*]oxazoles were replaced by 6-chloro or 6-fluoro-benzo[*d*]-thiazoles [(1*S*,6*R*)-**64** and (1*S*,6*R*)-**65**]. Unfortunately, these compounds were still moderate Pgp substrates with increased shifts in the time-dependent CYP3A4 inhibition as compared with **23a**. The most potent derivatives were obtained when the benzo[*d*]oxazole ring was replaced by the quinoxaline moiety [(1*S*,6*R*)-**66**]. We therefore investigated different substitution patterns on the quinoxaline skeleton in order to keep the strong potency on both receptors found for (1*S*,6*R*)-**66** yet minimizing the CYP3A4 shift and the affinity for Pgp. Representative modifications reported in Table 7 confirmed the strong affinity of the quinoxalines for the orexin receptors with potencies reached below 10 nM on both receptors [(1*S*,6*R*)-**67**, (1*S*,6*R*)-**71**, and (1*S*,6*R*)-**72**]. Unfortunately, the compounds were all strong Pgp substrates. At this stage, we started to suspect the 2*H*-1,2,3-triazole moiety to be part of the pharmacophore recognized by the Pgp resulting in high Pgp efflux values. To verify this hypothesis, we replaced the 1,2,3-triazole ring by 1*H*-pyrazole, 2-pyridine, or by a simple phenyl ring to study the impact on Pgp efflux ratio. In Table 8, we report some representative combinations.[47]

Interestingly for all compounds, we observed an orexin antagonist potency increase for R_1 = A < B < C antiparallel to the affinity for Pgp. Compounds bearing a pyrazole or a 2-pyridine ring as a replacement for the 1,2,3-triazole were similarly strong Pgp substrates, while compounds bearing a phenyl ring were poor Pgp substrates. This left us with five compounds fulfilling our criteria: (1*S*,6*R*)-**76c**, (1*S*,6*R*)-**79c**, (1*S*,6*R*)-**80c**, (1*S*,6*R*)-**81c**, and (1*S*,6*R*)-**82c**.

Figure 5 summarizes the BBB results of the five most promising compounds of Table 8. Based on these results we selected (1*S*,6*R*)-**80c** which was a highly brain penetrant compound ([B] = 2999 ng g^{-1}) with an excellent [B]/[P] ratio of 186% for further characterization.

Table 7. Representative isosteric replacements of 5-chlorobenzo[*d*]oxazole.

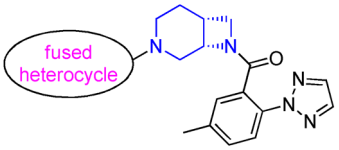

Fused heterocycle	Compd	IC_{50} [nM][a] hOx1	hOx2	HLM	CYP3A4 inhibition shift	Pgp efflux ratio
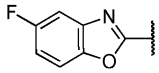	**63**	26	40	n.m.	n.m.	n.m.
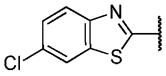	(1*S*,6*R*)-**64**	35	12	92	>4	4.8
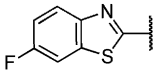	(1*S*,6*R*)-**65**	6.0	7.5	125	17	3.8
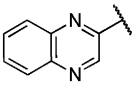	(1*S*,6*R*)-**66**	5.6	8	707	>19.6	n.m.
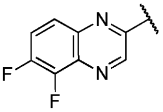	(1*S*,6*R*)-**67**	9.3	4.3	61	>2.4	29
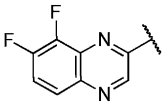	**68**	90	79	n.m.	n.m.	n.m.
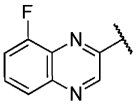	(1*S*,6*R*)-**69**	7.0	13	>1250	n.m.	n.m.
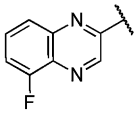	(1*S*,6*R*)-**70**	8.5	19	427	3.1	30
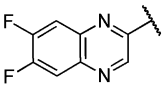	(1*S*,6*R*)-**71**	6.4	2.3	323	>2.3	9
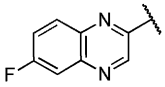	(1*S*,6*R*)-**72**	1.9	0.8	92	>2.8	16
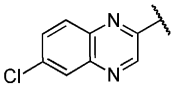	**73**	22	13	n.m.	n.m.	n.m.
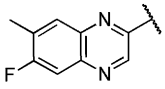	**74**	21	42	n.m.	n.m.	n.m.

[a] Values are the geometric mean of at least two to three independent experiments as determined by FLIPR assay (see the Supporting Information for details); n.m. = not measured.

For comparative purposes we prepared the corresponding regioisomers (1*R*,6*S*)-**83**, **84**, **85**, and **86** of compound **80c**. The data on HLM, shift in the time-dependent CYP3A4 inhibition and MDR1, reported in Table 9, show the same trend in potency and Pgp efflux ratios but indicate that compounds **83**, **84**, **85**, and **86** are highly unstable in HLM. This confirmed our initial choice to favor the (1*S*,6*R*)-3,8-diazabicyclo[4.2.0]octane regioisomer.

To provide large enough amounts of (1*S*,6*R*)-**80c** for full in vitro and in vivo characterization, an easily scalable synthesis was developed as illustrated in Scheme 2. The quinoxaline was synthesized in two steps starting from 4,5-difluorobenzene-1,2-diamine **87**. Condensation with glyoxylic acid followed by chlorination using $POCl_3$ afforded the 2-chloro-6,7-difluoroquinoxaline **89** in 81% over two steps. The 4-methyl-[1,1′-biphenyl]-2-carboxylic acid **94** was obtained in three steps starting

Table 8. Bioisosteric replacements for the 5-chlorobenzo[*d*]oxazole and the 2*H*-1,2,3-triazole.

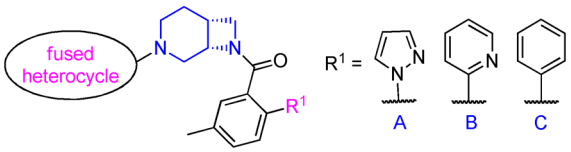

Fused heterocycle	R^1	Compd	IC_{50} [nM][a] hOx1	hOx2	HLM	CYP3A4 inhibition shift	Pgp efflux ratio
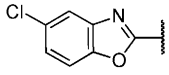	**A**	**75a**	53	132	n.m.	n.m.	n.m.
	B	**75b**	25	154	n.m.	n.m.	n.m.
	C	**75c**	9.2	26	n.m.	n.m.	n.m.
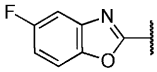	**A**	**76a**	31	152	n.m.	n.m.	n.m.
	B	(1*S*,6*R*)-**76b**	17	35	158	>3.8	12
	C	(1*S*,6*R*)-**76c**	4.0	6.8	276	3.2	1.6
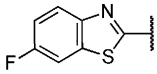	**A**	(1*S*,6*R*)-**77a**	20	15	242	23	n.m.
	B	(1*S*,6*R*)-**77b**	18	29	148	15	n.m.
	C	(1*S*,6*R*)-**77c**	4.4	4.8	181	9.3	n.m.
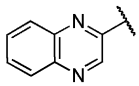	**A**	(1*S*,6*R*)-**78a**	9.4	26	606	>46	n.m.
	B	(1*S*,6*R*)-**78b**	n.m.	n.m.	n.m.	n.m.	n.m.
	C	(1*S*,6*R*)-**78c**	2.3	2.8	>1250	23	n.m.
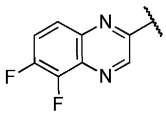	**A**	(1*S*,6*R*)-**79a**	36	12	139	>4	10
	B	(1*S*,6*R*)-**79b**	20	8.8	198	>4.5	17
	C	(1*S*,6*R*)-**79c**	3.9	1.4	196	4.6	3
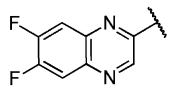	**A**	(1*S*,6*R*)-**80a**	17	4.0	363	5.1	8.5
	B	(1*S*,6*R*)-**80b**	14	6.5	489	4.5	8.5
	C	(1*S*,6*R*)-**80c**	4.5	1.3	336	2.9	1.7
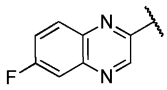	**A**	(1*S*,6*R*)-**81a**	11	4.8	193	>2.8	8.7
	B	(1*S*,6*R*)-**81b**	11	6.6	225	>2.2	14
	C	(1*S*,6*R*)-**81c**	2.0	1.3	375	2.6	2.9
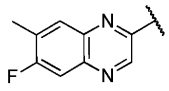	**A**	**82a**	114	173	n.m.	n.m.	n.m.
	B	**82b**	126	240	n.m.	n.m.	n.m.
	C	(1*S*,6*R*)-**82c**	12	17	383	3.8	1.8

[a] Values are the geometric mean of at least two to three independent experiments as determined by FLIPR assay (see the Supporting Information for details); n.m. = not measured.

Table 9. (1*R*,6*S*)-Regioisomers of (1*S*,6*R*)-**71**, (1*R*,6*S*)-**80a**, (1*R*,6*S*)-**80b**, and (1*R*,6*S*)-**80c**.

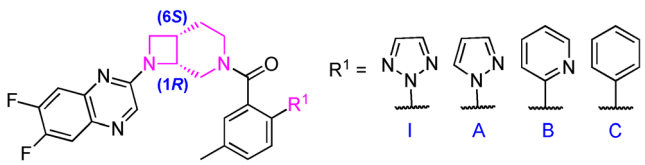

Fused heterocycle	R^1	Compd	IC_{50} [nM][a] hOx1	hOx2	HLM	CYP3A4 inhibition shift	Pgp efflux ratio
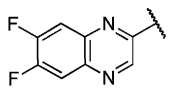	**I**	(1*R*,6*S*)-**83**	1.5	2.1	913	4.5	12
	A	(1*R*,6*S*)-**84**	2.0	7.5	605	12.3	8.6
	B	(1*R*,6*S*)-**85**	3.6	4.5	694	9.2	12
	C	(1*R*,6*S*)-**86**	1.1	1.4	893	4.9	1.2

[a] Values are the geometric mean of at least two to three independent experiments as determined by FLIPR assay (see the Supporting Information for details).

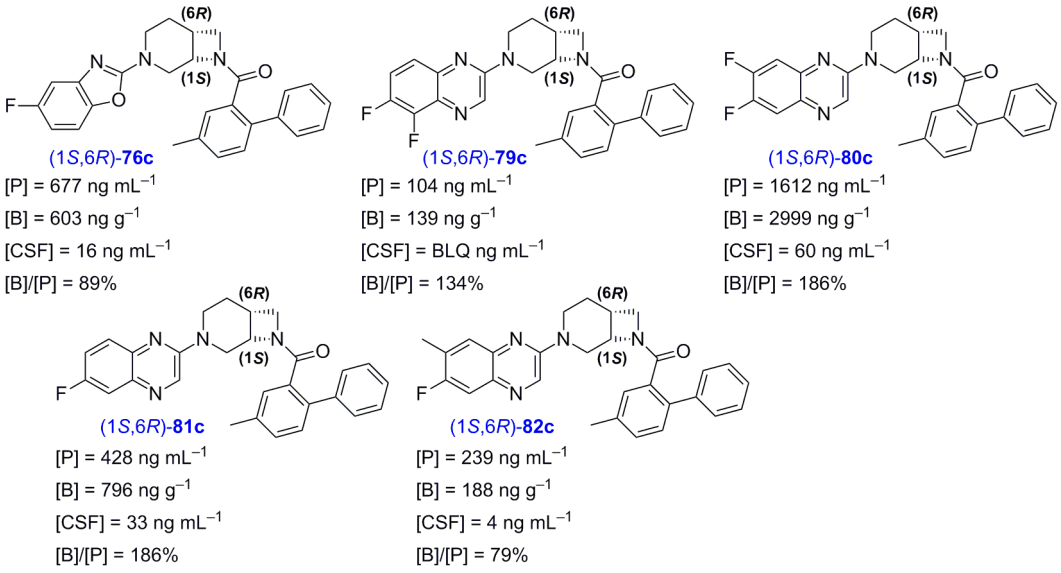

Figure 5. Structure–brain penetration analysis: BBB experiments performed in male Wistar rats after oral administration (100 mg kg^{-1} formulated in PEG 400; sampling at 3 h).

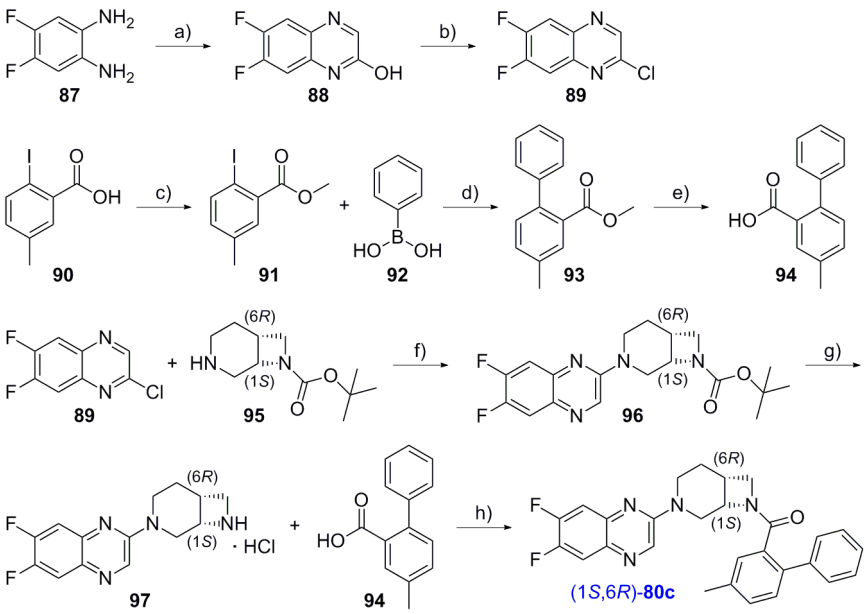

Scheme 2. Synthesis of DORA ((1*S*,6*R*)-3-(6,7-difluoroquinoxalin-2-yl)-3,8-diazabicyclo[4.2.0]octan-8-yl)(4-methyl-[1,1′-biphenyl]-2-yl)methanone **80c** (details given in the Supporting Information). *Reagents and conditions*: a) glyoxylic acid monohydrate, EtOH, reflux, 1 h, 86%; b) $POCl_3$, reflux, 30 min, 94%; c) H_2SO_4 conc. MeOH, reflux, 40 h, 99%; d) $Pd(PPh_3)_4$, Na_2CO_3 2 M, toluene, EtOH, 80 °C, 16 h, 86%; e) NaOH 32%, MeOH, 65 °C, 24 h, 88%; f) K_2CO_3, DMF, 60 °C, 2 h, 84%; g) HCl 4 N in dioxane, RT, 5 h, quant.; h) TBTU, DIPEA, CH_3CN, RT, 3 h, 80%.

from the commercially available 2-iodo-5-methylbenzoic acid **90**. Esterification followed by Suzuki coupling using phenylboronic acid **92** afforded the methyl 4-methyl-[1,1′-biphenyl]-2-carboxylate **93** that was further saponified yielding the desired acid **94** in 75% over three steps. *tert*-Butyl (1*S*,6*R*)-3,8-diazabicyclo[4.2.0]octane-8-carboxylate **95** was synthesized according to known procedures.[42] Nucleophilic aromatic substitution using 2-chloro-6,7-difluoroquinoxaline **89** followed by Boc-deprotection and amide coupling with 4-methyl-[1,1′-biphenyl]-2-carboxylic acid **94** yielded ((1*S*,6*R*)-3-(6,7-difluoroquinoxalin-2-yl)-3,8-diazabicyclo[4.2.0]octan-8-yl)(4-methyl-[1,1′-biphenyl]-2-yl)methanone **80c**.

The in vitro and in vivo data generated for (1*S*,6*R*)-**80c** are reported in Tables 10 and 11. Compound (1*S*,6*R*)-**80c** is a potent DORA not only on human but also on rat and dog receptors, with an excellent PSA (48.25 Å^2) and high passive permeability ($P_{app} = 34.10^{-6}$ cm s^{-1}). In line with its high lipophilicity, low free fractions in human, dog and rat plasma (0.2–0.4%),

Table 10. In vitro data generated with compound (1*S*,6*R*)-**80 c**.[a]

Properties	(1*S*,6*R*)-**80 c**
PhysChem properties	
M_r [g mol^{-1}]	470.52
Log$D_{7.4}$	4.7
PSA [Å^2]	48.25
Human, rat, and dog orexin receptors	
IC_{50} (hOx1/rOx1/dOx1) [nM]	4.5/8.8/13
IC_{50} (hOx2/rOx2/dOx2) [nM]	1.3/0.8/7.5
CYP inhibition	
IC_{50} (CYP3A4T) [μM]	11
IC_{50} (CYP3A4M) [μM]	18
CYP3A4 shift	2.9
IC_{50} (CYP2C9) [μM]	8.5
CYP2C9 shift	1
IC_{50} (CYP2D6) [μM]	37
CYP2D6 shift	1
Metabolic stability in liver microsomes	
HLM [μL min^{-1} mg^{-1}]	336
RLM [μL min^{-1} mg^{-1}]	>1250
DLM [μL min^{-1} mg^{-1}]	296
Plasma protein binding	
PPB [%] (human/rat/dog)	99.8/99.6/99.8
Fu_rat brain	0.001
MDR1 assay	
P_{app} A→B [10^{-6} cm s^{-1}]	20
P_{app} B→A [10^{-6} cm s^{-1}]	34
Efflux ratio	1.7

[a] Orexin activity data represent the geometric mean of at least two to three independent experiments and were determined by FLIPR assay (see the Supporting Information for details). CYP3A4T: testosterone as marker substrate; CYP3A4M: midazolam as marker substrate; HLM, RLM, and DLM values represent a normalized rate constant.

Table 11. In vivo data generated with compound (1*S*,6*R*)-**80 c**.[a]

Properties	(1*S*,6*R*)-**80 c**	
Pharmacokinetics: Wistar rat,[a,b] 1 mg kg^{-1} i.v.		
AUC [ng h mL^{-1}]	266	
CL [mL min^{-1} kg^{-1}]	63	
V_{ss} [L kg^{-1}]	3	
Terminal $t_{1/2}$ [h]	1.6	
Pharmacokinetics: rat,[a,b] 100 mg kg^{-1} p.o.		
AUC [ng h mL^{-1}]	6160	
C_{max} [ng mL^{-1}]	966	
t_{max} [h]	5	
F [%]	23	
Pharmacokinetics: Beagle dog,[a,b] 1 mg kg^{-1} i.v.		
AUC [ng h mL^{-1}]	1420	
CL [mL min^{-1} kg^{-1}]	12	
V_{ss} [L kg^{-1}]	3.9	
Terminal $t_{1/2}$ [h]	6.2	
Pharmacokinetics: Beagle dog[a,b]	**3 mg kg^{-1} p.o.**	**6.5 mg kg^{-1} p.o.**
AUC [ng h mL^{-1}]	611	1040
C_{max} [ng mL^{-1}]	108	237
t_{max} [h]	1.1	1.3
F [%]	11	16

[a] Data are the geometric mean; the median is given for t_{max}. [b] For formulation details, see the experimental section in the Supporting Information.

and in rat brain (0.1%) were measured. No liability on CYP inhibition could be identified and the compound was not a Pgp substrate. It showed moderate stability in HLM and in DLM, which is favorable for a sleeping drug. Also consistent with its high intrinsic clearance in RLM (>1250 μL min^{-1} mg^{-1}), (1*S*,6*R*)-**80 c** showed a high clearance in Wistar rats (63 mL min^{-1} kg^{-1}). The volume of distribution at steady-state (V_{ss}) as a general measure of tissue distribution, was 3.0 L kg^{-1} exceeding total body water volume and indicating significant distribution in tissues. In vivo pharmacokinetics were determined in male Wistar rats and in male Beagle dogs. To overcome the high clearance and allow sufficient exposure for the in vivo pharmacology in Wistar rats, the oral PK was performed at 100 mg kg^{-1}. The AUC (6160 ng h mL^{-1}, rat) and oral bioavailability (23%, rat) obtained under these experimental conditions

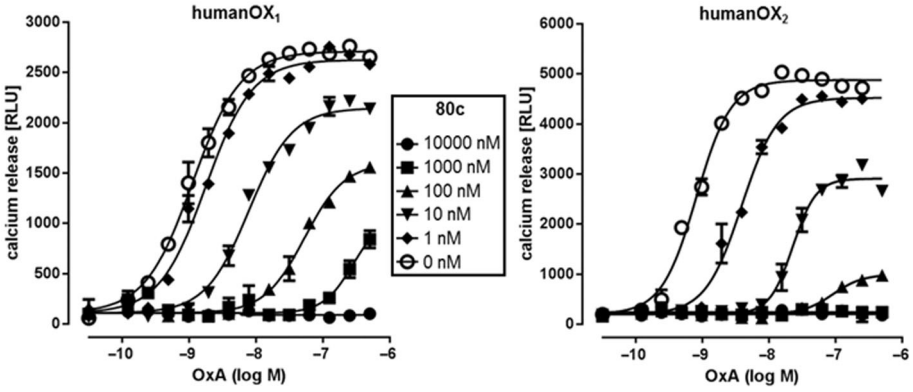

Figure 6. Effect of (1*S*,6*R*)-**80 c** on OXA-induced calcium release. CHO cells expressing either the human Ox1 or human Ox2 receptor were pre-incubated with dilution series of **80 c** for 120 min followed by the addition of a dilution series of OxA. Calcium release was recorded, peak fluorescence values were exported, and concentration–response curves were generated. IC_{50} values at 3.9 nM OxA were determined and used as a basis to calculate the apparent K_b via the generalized Cheng–Prusoff equation. Shown is one out of $n=2$ identical experiments. Values represent arithmetic mean of duplicates ± SD.

were acceptable for a broad in vivo pharmacological characterization in rats as well as in dogs (see Table 11).

The mode of antagonism of (1*S*,6*R*)-**80 c** at Ox1R and Ox2R was assessed in more detail using a Ca^{2+} release assay with stably transfected Chinese hamster ovary (CHO) cells recombinantly expressing human Ox1 or Ox2 receptors. Orexin A concentration–response curves (CRC) were generated in the presence of increasing concentrations of (1*S*,6*R*)-**80 c** (Figure 6). The compound induced rightward shifts of the OXA CRCs and a suppression of the maximal OXA response demonstrating insurmountable antagonism.[48] Apparent K_b values (an approximation of the inhibitory constant if IC_{50} values generated at low agonist concentrations are used) were thus calculated with the help of the generalized Cheng–Prusoff equation as described in the Supporting Information. Apparent K_b values for 120 min antagonist pre-incubation were calculated to be $K_b = 1$ nM (human Ox1) and 0.32 nM (human Ox2).

With the reasonable rat pharmacokinetics at 100 mg kg^{-1} in PEG400, the high brain exposure reached under the same conditions ([B] = 2999 ng g^{-1}) and the favorable insurmountable antagonistic profile on both receptors, the effect on sleep promotion of (1*S*,6*R*)-**80 c** was assessed as previously described for **22 a** and **23 b**. At a single oral dose of 100 mg kg^{-1}, (1*S*,6*R*)-**80 c** significantly decreased by 32% the home cage activity over the 12 h night period following administration relative to vehicle-treated rats ($p < 0.01$, paired *t*-test; Figure 7). Based on electrophysiological parameters, it significantly decreased (16%) the time spent in active wake compared with vehicle-treated rats ($p < 0.01$, paired *t*-test). The time spent in quiet wake was nearly unchanged (−3% relative to vehicle-treated rats, $p > 0.05$, paired *t*-test). By compensation, the time spent in non-REM and REM sleep was significantly increased by 14 and 42% respectively compared with vehicle-treated rats ($p < 0.01$ for both, paired *t*-test). The total sleeping time was increased by 18% compared with vehicle-treated rats. The effects observed were similar to benchmark compound **3** (Figure 4).

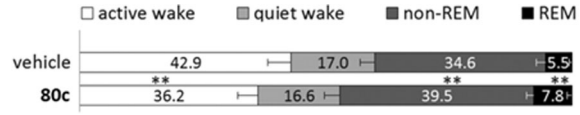

Figure 7. Effect of (1*S*,6*R*)-**80 c** on the time spent in sleep and wake stages (percent of total time) during the 12 h night active period following administration in male Wistar rats. Rats were administered a single oral dose of vehicle or 100 mg kg^{-1} of compound. Data are presented as mean ± SEM; $^{*}p < 0.05$, $^{**}p < 0.01$ ($n = 8$).

Based on these results and the encouraging PK in Beagle dogs, we further tested the compound in male Beagle dogs with single oral dose of 30, 100 and 300 mg total dose formulated in mannitol capsules ($n = 7$; experiment done in a crossover design). The animals were treated in the morning during their active phase. Over the 9-hour daylight period following administration, the compound dose-dependently decreased electrophysiological signs of wakefulness (time spent in active wake; one-way ANOVA, $p < 0.001$; Figure 8). (1*S*,6*R*)-**80 c** dose

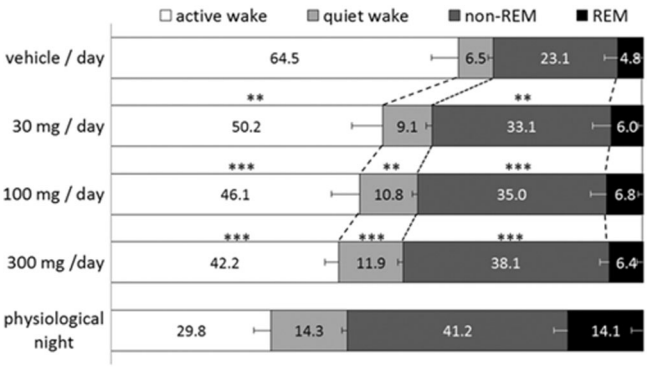

Figure 8. Effect of (1*S*,6*R*)-**80 c** on the time spent in sleep and wake stages (percent of total time) during 9 h of active period following administration in male Beagle dogs ($n = 7$; experiment done in a crossover design). Dogs were administered a single oral dose of vehicle or (1*S*,6*R*)-**80 c** at 30, 100 or 300 mg in the daytime. Data are presented as mean ± SEM; Dunnett post-hoc analysis: $^{**}p < 0.01$, $^{***}p < 0.001$ ($n = 7$).

dependently increased the time spent in non-REM sleep (one-way ANOVA; $p < 0.001$) and in quiet wake (one-way ANOVA; $p < 0.01$). The first significant effects were already observed at the dose of 30 mg/dog. The time spent in REM sleep was not significantly increased (one-way ANOVA, $p > 0.05$). Vehicle-treated dogs slept in total 28% of the 9-hour daylight period following administration, divided into 84% non-REM sleep and 16% REM sleep. At the highest dose tested (300 mg/dog), the relative proportion of time spent in non-REM and REM sleep stayed similar with dogs sleeping in total 44% of the time, divided in 86% non-REM sleep and 14% REM sleep (one-way ANOVA, $p > 0.05$).

With those results, we further profiled the compound to prepare it for preclinical candidate selection. It was shown not to be mutagenic in the AMES test but our excitement over the favorable attributes of (1*S*,6*R*)-**80 c** ended with the discovery that it was highly phototoxic with a photo-irritancy factor (PIF) of 44 and an ED_{50} of 190 ng mL^{-1} (0.4 μM), which is in the range of plasma concentrations achieved in vivo.[49] These data and the fact that two patent applications that cover our own series appeared in literature prompted us to suspend further studies of this compound class.[46,47,50]

Conclusions

In summary, we have identified new DORAs following a scaffold-hopping approach using **3** as a template. The replacement of the initial ring with "in principle equally suited" scaffolds led to marked differences in activity, and even within one structural class, fine tuning was necessary to obtain optimal overall properties. Among the different possible starting points, we decided to pursue with the 3,8-diazabicyclo[4.2.0]octane template for SAR optimization. The insurmountable highly brain penetrant DORA **80 c** was broadly characterized for physicochemical and pharmacokinetic properties as well as in in vivo pharmacological models. The sleep-promoting effect of **80 c** was similar to the effect observed with suvorexant **3**. In vitro

phototoxicity prevented us from further pursuing with this compound.

Acknowledgements

The authors thank Daniel Hafner, Elise Salomé, Daniel Marchal, Katalin Menyhart, Celia Müller-Grandjean, Thomas Sasse, Cédric Fischer, Hélène Roellinger, Hélène Massinet, Wenyu Wang, Changbin Qui, Stephane Delahaye, Isabelle Weber, Fabienne Drouet, Rolf Wuest, Julia Friedrich, Stephanie Hertzog, Päivi Aänismaa, Markus van Raumer, Bruno Capeleto, Patrick Bouis, Elise Jacob, Pascal Fullhardt, Christine Metzger, Sandrine Chopinet, Amandine Fraichard, Kristina Kamin, and Mourad Nabate. Special thanks to Thomas Weller for his support, his enthusiasm, and for the stimulating discussions.

Keywords: drug design · orexin receptor antagonists · scaffold hopping · sleep disorders · structure–activity relationships

[1] S. Passarella, M.-T. Duong, *Am. J. Health-Syst. Pharm.* **2008**, *65*, 927 – 934.
[2] M. Daley, C. M. Morin, M. LeBlanc, J. P. Gregoire, J. Savard, L. Baillargeo, *Sleep Med.* **2009**, *10*, 427 – 438.
[3] a) S. S. Sullivan, C. Guilleminault, *Expert Opin. Emerging Drugs* **2009**, *14*, 411 – 422; b) J. J. Renger, *Curr. Top. Med. Chem.* **2008**, *8*, 937 – 953.
[4] K. A. Wafford, B. Ebert, *Nat. Rev. Drug Discovery* **2008**, *7*, 530 – 540.
[5] a) T. Sakurai, A. Amemiya, M. Ishii, I. Matsuzaki, R. M. Chemelli, H. Tanaka, S. C. Williams, J. A. Richardson, G. P. Kozlowski, S. Wilson, J. R. S. Arch, R. E. Buckingham, A. C. Haynes, S. A. Carr, R. S. Annan, D. E. McNulty, W. Liu, J. A. Terrett, N. A. Elshourbagy, D. J. Bergsma, M. Yanagisawa, *Cell* **1998**, *92*, 573 – 585; b) L. de Lecea, T. S. Kilduff, C. Peyron, X.-B. Gao, P. E. Foye, P. E. Danielson, C. Fukuhara, E. L. Battenberg, V. T. Gautvik, F. S. Bartlett II, W. N. Frankel, A. N. van den Pol, F. E. Bloom, K. M. Gautvik, J. G. Sutcliffe, *Proc. Natl. Acad. Sci. USA* **1998**, *95*, 322 – 327.
[6] C. Peyron, D. K. Tighe, A. N. van den Pol, L. de Lecea, H. C. Heller, J. G. Sutcliffe, T. S. Kilduff, *J. Neurosci.* **1998**, *18*, 9996 – 10015.
[7] For a compilation of the extensive investigations carried out to identify the orexin system and define its physiological roles, see: *Hypocretins: Integrators of Physiological Functions* (Eds.: L. de Lecea, J. G. Sutcliffe), Springer, New York, **2005**.
[8] S. Nishino, *Sleep Med.* **2007**, *8*, 373 – 399.
[9] a) C. Boss, C. Brisbare-Roch, F. Jenck, *J. Med. Chem.* **2009**, *52*, 891 – 902; b) C. Boss, C. Brisbare-Roch, F. Jenck, H. Aissaoui, R. Koberstein, T. Sifferlen, T. Weller, *Chimia* **2008**, *62*, 974 – 979; c) A. J. Roecker, P. J. Coleman, *Curr. Top. Med. Chem.* **2008**, *8*, 977 – 987; d) J. Gatfield, C. Brisbare-Roch, F. Jenck, C. Boss, *ChemMedChem* **2010**, *5*, 1197 – 1214.
[10] a) D. Smart, J. C. Jerman, *Pharmacol. Ther.* **2002**, *94*, 51; b) C. R. Baumann, C. L. Bassetti, *Lancet Neurol.* **2005**, *4*, 673 – 682.
[11] M. J. Bingham, J. Cai, M. R. Deehan, *Curr. Opin. Drug Discovery Dev.* **2006**, *9*, 551 – 559.
[12] a) T. Mochizuki, A. Crocker, S. McCormack, M. Yanagisawa, T. Sakurai, T. E. Scammell, *J. Neurosci.* **2004**, *24*, 6291 – 6300; b) R. M. Chemelli, J. T. Willie, C. M. Sinton, J. K. Elmquist, T. Scammell, C. Lee, J. A. Richardson, S. C. Williams, Y. Xiong, Y. Kisanuki, T. E. Fitch, M. Nakazato, R. E. Hammer, C. B. Saper, M. Yanagisawa, *Cell* **1999**, *98*, 437 – 451.
[13] a) A. S. Foutz, M. M. Mitler, L. L. Cavalli-Sforza, W. C. Dement, *Sleep* **1979**, *1*, 413 – 421; b) J. Riehl, S. Nishino, R. Cederberg, W. C. Dement, E. Mignot, *Exp. Neurol.* **1998**, *152*, 292 – 302.
[14] C. Peyron, J. Faraco, W. Rogers, B. Ripley, S. Overeem, Y. Charnay, S. Nevsimalova, M. Aldrich, D. Reynolds, R. Albin, R. Li, M. Hungs, M. Pedrazzoli, M. Padigaru, M. Kucherlapati, J. Fan, R. Maki, G. J. Lammers, C. Bouras, R. Kucherlapati, S. Nishino, E. A. Mignot, *Nat. Med.* **2000**, *6*, 991 – 997.
[15] J. Cai, F. E. Cooke, B. S. Sherborne, *Expert Opin. Ther. Pat.* **2006**, *16*, 631 – 646.
[16] C. Brisbare-Roch, J. Dingemanse, R. Koberstein, P. Hoever, H. Aissaoui, S. Flores, C. Mueller, O. Nayler, J. van Gerven, S. L. de Haas, P. Hess, C. Qiu, S. Buchmann, M. Scherz, T. Weller, W. Fischli, M. Clozel, F. Jenck, *Nat. Med.* **2007**, *13*, 150 – 155.
[17] D. N. Neubauer, *Curr. Opin. Invest. Drugs* **2010**, *11*, 101 – 110.
[18] C. D. Cox, M. J. Breslin, D. B. Whitman, J. D. Schreier, G. B. McGaughey, M. J. Bogusky, A. J. Roecker, S. P. Mercer, R. A. Bednar, W. Lemaire, J. G. Bruno, D. R. Reiss, C. M. Harrell, K. L. Murphy, S. L. Garson, S. M. Doran, T. Prueksaritanont, W. B. Anderson, C. Tang, S. Roller, T. D. Cabalu, D. Cui, G. D. Hartman, S. D. Young, K. S. Koblan, C. J. Winrow, J. J. Renger, P. J. Coleman, *J. Med. Chem.* **2010**, *53*, 5320 – 5332.
[19] P. J. Coleman, C. D. Cox, A. J. Roecker, *Curr. Top. Med. Chem.* **2011**, *11*, 696 – 725.
[20] P. Hoever, P. G. Dorffner, H. Benes, T. Penzel, H. Danker-Hopfe, M. J. Barbanoj, G. Pillar, B. Saletu, O. Polo, D. Kunz, J. Zeitlhofer, S. Berg, M. Partinen, C. L. Bassetti, B. Hçgl, I. O. Ebrahim, E. Holsboer-Trachsler, H. Bengtsson, Y. Peker, U. M. Hemmeter, E. Chiossi, G. Hajak, J. Dingemanse, *Clin. Pharmacol. Ther.* **2012**, *91*, 975 – 985.
[21] D. Michelson, E. Snyder, E. Paradis, M. Chengan-Liu, D. B. Snavely, J. Hutzelmann, J. K. Walsh, A. D. Krystal, R. M. Benca, M. Cohn, C. Lines, T. Roth, W. J. Herring, *Lancet Neurol.* **2014**, *13*, 461 – 471.
[22] C. J. Winrow, J. J. Renger, *Br. J. Pharmacol.* **2014**, *171*, 283 – 293.
[23] Y. Zhu, Y. Miwa, A. Yamanaka, T. Yada, M. Shibahara, Y. Abe, T. Sakurai, K. Goto, *J. Pharmacol. Sci.* **2003**, *92*, 259 – 266.
[24] L. Lin, J. Faraco, R. Li, H. Kadotani, W. Rogers, X. Lin, X. Qiu, P. J. de Jong, S. Nishino, E. Mignot, *Cell* **1999**, *98*, 365 – 376.
[25] S. Nishino, B. Ripley, S. Overeem, G. J. Lammers, E. Mignot, *Lancet* **2000**, *355*, 39 – 40.
[26] P. Bettica, L. Squassante, S. Zamuner, G. Nucci, H. Danker-Hopfe, E. Ratti, *Sleep* **2012**, *35*, 1097 – 1104.
[27] L. Citrome, *Int. J. Clin. Pract.* **2014**, *68*, 1429 – 1441.
[28] Belsomra US Package Insert, United States Food and Drug Administration product information. Available from: www.accessdata.fda.gov/scripts/cder/drugsatfda/index.cfm?fuseaction=Search.Label_ApprovalHistory#labelinfo.
[29] T. Sifferlen, C. Boss, E. Cottreel, R. Koberstein, M. Gude, H. Aissaoui, T. Weller, J. Gatfield, C. Brisbare-Roch, F. Jenck, *Bioorg. Med. Chem. Lett.* **2010**, *20*, 1539 – 1542.
[30] H. Aissaoui, R. Koberstein, C. Zumbrunn, J. Gatfield, C. Brisbare-Roch, F. Jenck, A. Treiber, C. Boss, *Bioorg. Med. Chem. Lett.* **2008**, *18*, 5729 – 5733.
[31] T. Sifferlen, R. Koberstein, E. Cottreel, A. Boller, T. Weller, J. Gatfield, C. Brisbare-Roch, F. Jenck, C. Boss, *Bioorg. Med. Chem. Lett.* **2013**, *23*, 3857 – 3863.
[32] J. T. Williams, J. Gatfield, C. Roch, A. Treiber, F. Jenck, M. H. Bolli, C. Brotschi, T. Sifferlen, B. Heidmann, C. Boss, *MedChemComm* **2015**, *6*, 1054 – 1064.
[33] T. Sifferlen, A. Boller, A. Chardonneau, E. Cottreel, J. Hoecker, H. Aissaoui, J. T. Williams, C. Brotschi, B. Heidmann, R. Siegrist, J. Gatfield, A. Treiber, C. Brisbare-Roch, F. Jenck, C. Boss, *Bioorg. Med. Chem. Lett.* **2014**, *24*, 1201 – 1208.
[34] T. Sifferlen, A. Boller, A. Chardonneau, E. Cottreel, J. Gatfield, A. Treiber, C. Roch, F. Jenck, H. Aissaoui, J. T. Williams, C. Brotschi, B. Heidmann, R. Siegrist, C. Boss, *Bioorg. Med. Chem. Lett.* **2015**, *25*, 1884 – 1891.
[35] C. Boss, C. Roch-Brisbare, M. A. Steiner, A. Treiber, H. Dietrich, F. Jenck, M. von Raumer, T. Sifferlen, C. Brotschi, B. Heidmann, J. T. Williams, H. Aissaoui, R. Siegrist, J. Gatfield, *ChemMedChem* **2014**, *9*, 2486 – 2496.
[36] P. Malherbe, O. Roche, A. Marcuz, C. Kratzeisen, J. G. Wettstein, C. Bissantz, *Mol. Pharmacol.* **2010**, *78*, 81 – 93.
[37] d.-T. Tran, P. Bonaventure, M. Hack, T. Mirzadegan, C. Dvorak, M. Letavic, N. Carruthers, T. Lovenberg, S. W. Sutton, *Eur. J. Pharmacol.* **2011**, *667*, 120 – 128.
[38] A. Heifetz, G. B. Morris, P. C. Biggin, O. Barker, T. Fryatt, J. Bentley, D. Hallett, D. Manikowski, S. Pal, R. Reifegerste, M. Slack, R. Law, *Biochemistry* **2012**, *51*, 3178 – 3197.
[39] D. B. Whitman, C. D. Cox, M. J. Breslin, K. M. Brashear, J. D. Schreier, M. J. Bogusky, R. A. Bednar, W. Lemaire, J. G. Bruno, G. D. Hartman, D. R. Reiss, C. M. Harrell, R. L. Kraus, Y. Li, S. L. Garson, S. M. Doran, T. Prueksaritanont, C. Li, C. J. Winrow, K. S. Koblan, J. J. Renger, P. J. Coleman, *ChemMedChem* **2009**, *4*, 1069 – 1074.
[40] P. J. Coleman, J. D. Schreier, C. D. Cox, M. J. Breslin, D. B. Whitman, M. J. Bogusky, G. B. McGaughey, R. A. Bednar, W. Lemaire, S. M. Doran, S. V. Fox, S. L. Garson, A. L. Gotter, C. M. Harell, D. R. Reiss, T. D. Cabalu, D. Cui, T. Prueksaritanont, J. Stevens, P. L. Tannenbaum, R. G. Ball, J. Stella-

bott, S. D. Young, G. D. Hartman, C. J. Winrow, J. J. Renger, *ChemMedChem* **2012**, *7*, 415 – 424.

[41] a) C. D. Cox, G. B. McGaughey, M. J. Bogusky, D. B. Whitman, R. G. Ball, C. J. Winrow, J. J. Renger, P. J. Coleman, *Bioorg. Med. Chem. Lett.* **2009**, *19*, 2997 – 3001; b) P. J. Coleman, J. D. Schreier, G. B. McGaughey, M. J. Bogusky, C. D. Cox, G. D. Hartman, R. G. Ball, C. M. Harrell, D. R. Reiss, T. Prueksaritonont, C. J. Winrow, J. J. Renger, *Bioorg. Med. Chem. Lett.* **2010**, *20*, 2311 – 2315.

[42] J. M. Frost née Pac, W. H. Bunnelle, K. R. Tietje, D. J. Anderson, L. E. Rueter, P. Curzon, C. S. Surowy, J. Ji, J. F. Daanen, K. L. Kohlhaas, M. J. Buckley, R. F. Henry, T. Dyhring, P. K. Ahring, M. D. Meyer, *J. Med. Chem.* **2006**, *49*, 7843 – 7853.

[43] For SAR around 3,7-diazabicyclo[3.3.1]nonane and 9-oxa-3,7-diazabicyclo[3.3.1]nonane, see: C. Boss, C. Brotschi, B. Heidmann, T. Sifferlen, J. T. Williams (Actelion Pharmaceuticals Ltd.), Int. PCT Pub. No. WO2013050938 A1, **2013**.

[44] Racemic **22** was resolved on a chiral Daicel ChiralPak IC HPLC column (5 μm; 20×250 mm) eluting with heptane/EtOH + 0.1% DIEA 50:50 at a flow rate of 16 mL min^{-1}. The first eluting enantiomer (**22a**) has a retention time of t_R = 10.73 min, and the second eluting enantiomer (**22b**) has a retention time of t_R = 14.18 min.

[45] Racemic **23** was resolved on a chiral Daicel ChiralPak IA HPLC column (5 μm; 30×250 mm) eluting with CH_3CN/MeOH + 0.1% DIEA 95:5 at a flow rate of 34 mL min^{-1}. The first eluting enantiomer (**23a**) has a retention time of t_R = 8.62 min, and the second eluting enantiomer (**23b**) has a retention time of t_R = 11.90 min.

[46] Some SAR work was also later performed using the core template (1*R*,6*S*)-3,8-diazabicyclo[4.2.0]octane with amide at the piperidine ring and aromatic systems at the azetidine ring. As feared, all interesting compounds showed high CYP3A4 time-dependent shift and/or were prone to be strong Pgp substrates. The same observations were made with the 3,6-diazabicyclo[3.2.0]heptane core template: C. Boss, C. Brotschi, B. Heidmann, T. Sifferlen, J. T. Williams (Actelion Pharmaceuticals Ltd.), Int. PCT Pub. No. WO2012085857 A1, **2012**.

[47] For a more exhaustive overview of the SAR using the core template (1*S*,6*R*)-3,8-diazabicyclo[4.2.0]octane with amide at the azetidine ring and aromatic systems at the piperidine ring, see: C. Boss, C. Brotschi, B. Heidmann, T. Sifferlen, J. T. Williams (Actelion Pharmaceuticals Ltd>), Int. PCT Pub. No. WO2012085852 A1, **2012**.

[48] A. L. Gotter, C. J. Winrow, J. Brunner, S. L. Garson, S. V. Fox, J. Binns, C. M. Harrell, D. Cui, K. L. Yee, M. Stiteler, J. Stevens, A. Savitz, P. L. Tannenbaum, S. J. Tye, T. McDonald, L. Yao, S. D. Kuduk, J. Uslaner, P. J. Coleman, J. J. Rengen, *BMC Neurosci.* **2013**, *14*, 90.

[49] The compound was tested in the NRU3T3 in vitro assay using chlorpromazine as positive control. A compound in this assay is flagged as phototoxic for PIF values exceeding 5. The PIF value for chlorpromazine in this assay is 23.

[50] B. J. Branstetter, M. A. Letavic, K. S. Ly, D. A. Rudolph, B. M. Savall, C. R. Shah, B. T. Shireman (Janssen Pharmaceutica NV), Int. PCT Pub. Nos. WO2011050200 A1 and WO2011050202 A1.

Received: March 29, 2016
Revised: May 18, 2016
Published online on ■■ ■■, 0000

B. Heidmann, J. Gatfield, C. Roch, A. Treiber, S. Tortoioli, C. Brotschi, J. T. Williams, M. H. Bolli, S. Abele, T. Sifferlen, F. Jenck, C. Boss*

■■ – ■■

Discovery of Highly Potent Dual Orexin Receptor Antagonists via a Scaffold-Hopping Approach

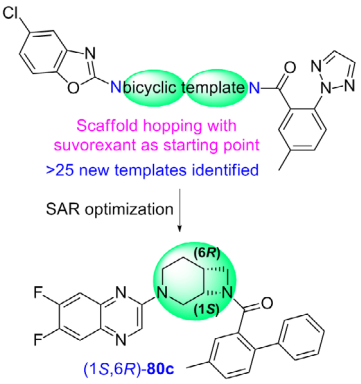

Scaffold hopping for hits: Dual orexin receptor antagonism has been shown to be a new mechanism for the treatment of primary insomnia and other sleep-related disorders. We report a scaffold-hopping approach as a powerful tool to identify high-quality hits as well as the structural optimization of one scaffold into **80 c**, a potent and orally bioavailable brain-penetrant dual orexin receptor antagonist.